Supplementary material for

MINIMAL SURFACES ON MIRROR-SYMMETRIC FRAMES. FLUID DYNAMICS ANALOGY

Mars M.Alimov[1], Alexander V.Bazilevsky[2] and Konstantin G.Kornev[3].
[1]Kazan Federal University, Kazan, Russia
[2] Ishlinsky Institute for Problems in Mechanics, Russian Academy of Sciences, Moscow, Russia
[2]Department of Materials Science and Engineering, Clemson University, Clemson, SC, 29634–0971, USA

1. Relating the partial derivatives $\partial x/\partial h$, $\partial y/\partial h$ and $\partial x/\partial \psi$, $\partial y/\partial \psi$ to the $\theta(h,\psi)$ and $J(h,\psi)$ functions.

To transform eq. (3.5),

$$\begin{aligned} \frac{\partial h}{\partial x} &= -\Phi(J)\cos\theta, \qquad \frac{\partial h}{\partial y} = -\Phi(J)\sin\theta, \\ \frac{\partial \psi}{\partial x} &= -J\sin\theta, \qquad \frac{\partial \psi}{\partial y} = J\cos\theta, \end{aligned} \tag{S.1}$$

into the Cauchy-Riemann equations (3.8), we write the exact differentials of functions $h(x,y)$ and $\psi(x,y)$ as

$$dh = \frac{\partial h}{\partial x}dx + \frac{\partial h}{\partial y}dy, \quad d\psi = \frac{\partial \psi}{\partial x}dx + \frac{\partial \psi}{\partial y}dy.$$

Using eqs. (S.1), these exact differentials are written in the form

$$dh = -\Phi(J)\cos\theta\, dx - \Phi(J)\sin\theta dy; \qquad d\psi = -J\sin\theta dx + J\cos\theta dy. \tag{S.2}$$

To express functions $x(h,\psi)$, $y(h,\psi)$ in terms of the variables h,ψ, we solve linear eqs. (S.2) for dx, dy to obtain

$$dx = -\frac{\cos\theta}{\Phi(J)}dh - \frac{\sin\theta}{J}d\psi, \qquad dy = -\frac{\sin\theta}{\Phi(J)}dh + \frac{\cos\theta}{J}d\psi. \tag{S.3}$$

Consequently, from these exact differentials (S.3), the partial derivatives of $x(h,\psi)$, $y(h,\psi)$ with respect to variables h,ψ, are found as

$$\begin{aligned} \frac{\partial x}{\partial h} &= -\frac{\cos\theta}{\Phi(J)}, \qquad \frac{\partial y}{\partial h} = -\frac{\sin\theta}{\Phi(J)}, \\ \frac{\partial x}{\partial \psi} &= -\frac{\sin\theta}{J}, \qquad \frac{\partial y}{\partial \psi} = \frac{\cos\theta}{J}. \end{aligned} \tag{S.4}$$

These equations constitute the first step in the derivation of the Cauchy-Riemann equations (3.8).

2. Expressing $\theta(h,\psi)$ and $J(h,\psi)$ in variables h and ψ.

Following Chaplygin[1, 2] and squaring each equation of the first line of (S.4) and summing them, we have

$$\left(\frac{\partial x}{\partial h}\right)^2+\left(\frac{\partial y}{\partial h}\right)^2=\frac{1}{\Phi^2(J)},\qquad \left(\frac{\partial x}{\partial \psi}\right)^2+\left(\frac{\partial y}{\partial \psi}\right)^2=\frac{1}{J^2}. \tag{S.5}$$

The ratios of each pair of eqs. in (S.4) give:

$$\frac{\partial y}{\partial h}\Big/\frac{\partial x}{\partial h}=\tan(\theta),\quad \frac{\partial x}{\partial \psi}\Big/\frac{\partial y}{\partial \psi}=-\tan(\theta),$$

or

$$\theta=\arctan\left(\frac{\partial y}{\partial h}\Big/\frac{\partial x}{\partial h}\right)=-\arctan\left(\frac{\partial x}{\partial \psi}\Big/\frac{\partial y}{\partial \psi}\right). \tag{S.6}$$

Now, the idea is to relate the derivatives $\partial\theta/\partial\psi$, $\partial\theta/\partial h$ to $\partial J/\partial\psi$ and $\partial J/\partial h$ using eqs. (S.6) and (S.5). Differentiating the first eq. (S.6) with respect to ψ, we have

$$\frac{\partial\theta}{\partial\psi}=\frac{\left(\frac{\partial x}{\partial h}\right)^2}{\left(\frac{\partial x}{\partial h}\right)^2+\left(\frac{\partial y}{\partial h}\right)^2}\left[\frac{\partial^2 y}{\partial h\partial\psi}\left(\frac{\partial x}{\partial h}\right)^{-1}-\frac{\partial y}{\partial h}\left(\frac{\partial x}{\partial h}\right)^{-2}\frac{\partial^2 x}{\partial h\partial\psi}\right].$$

Then, using the first eq. (S.5), we finally write

$$\frac{\partial\theta}{\partial\psi}=\Phi^2(J)\left[\frac{\partial^2 y}{\partial h\partial\psi}\left(\frac{\partial x}{\partial h}\right)-\frac{\partial^2 x}{\partial h\partial\psi}\left(\frac{\partial y}{\partial h}\right)\right]. \tag{S.7}$$

Differentiating the second eq. (S.6) with respect to h, we obtain

$$\frac{\partial\theta}{\partial h}=\frac{-\left(\frac{\partial y}{\partial \psi}\right)^2}{\left(\frac{\partial y}{\partial \psi}\right)^2+\left(\frac{\partial x}{\partial \psi}\right)^2}\left[\frac{\partial^2 x}{\partial\psi\partial h}\left(\frac{\partial y}{\partial\psi}\right)^{-1}-\frac{\partial x}{\partial\psi}\left(\frac{\partial y}{\partial\psi}\right)^{-2}\frac{\partial^2 y}{\partial\psi\partial h}\right].$$

Then, using the second eq. (S.5), we have

$$\frac{\partial\theta}{\partial h}=-J^2\left[\frac{\partial^2 x}{\partial\psi\partial h}\left(\frac{\partial y}{\partial\psi}\right)-\frac{\partial^2 y}{\partial\psi\partial h}\left(\frac{\partial x}{\partial\psi}\right)\right]. \tag{S.8}$$

Replacing $\partial x/\partial h$, $\partial y/\partial h$ in (S.7) by their expressions from the first line of eqs. (S.4), and replacing $\partial x/\partial\psi$, $\partial y/\partial\psi$ in (S.8) by their expressions from the second line of eqs. (S.4), we get

$$\frac{1}{\Phi(J)}\frac{\partial\theta}{\partial\psi}=\sin\theta\frac{\partial^2 x}{\partial h\partial\psi}-\cos\theta\frac{\partial^2 y}{\partial h\partial\psi},\tag{S.9}$$

$$\frac{1}{J}\frac{\partial\theta}{\partial h}=-\cos\theta\frac{\partial^2 x}{\partial\psi\partial h}-\sin\theta\frac{\partial^2 y}{\partial\psi\partial h}.\tag{S.10}$$

Analogously, differentiating the first eq. (S.5) with respect to ψ, and the second eq. (S.5) with respect to h, we have

$$-2\frac{\Phi'(J)}{\Phi^3(J)}\frac{\partial J}{\partial\psi}=2\frac{\partial^2 x}{\partial h\partial\psi}\left(\frac{\partial x}{\partial h}\right)+2\frac{\partial^2 y}{\partial h\partial\psi}\left(\frac{\partial y}{\partial h}\right),\tag{S.11}$$

$$-2\frac{1}{J^3}\frac{\partial J}{\partial h}=2\frac{\partial^2 x}{\partial\psi\partial h}\left(\frac{\partial x}{\partial\psi}\right)+2\frac{\partial^2 y}{\partial\psi\partial h}\left(\frac{\partial y}{\partial\psi}\right).\tag{S.12}$$

Similarly replacing $\partial x/\partial h$, $\partial y/\partial h$ in (S.11) by their expressions from the first line of eqs. (S.4), and replacing $\partial x/\partial\psi$, $\partial y/\partial\psi$ in (S.12) by their expressions from the second line of eqs. (S.4), we get

$$-\frac{\Phi'(J)}{\Phi^2(J)}\frac{\partial J}{\partial\psi}=-\cos\theta\frac{\partial^2 x}{\partial h\partial\psi}-\sin\theta\frac{\partial^2 y}{\partial h\partial\psi},\tag{S.13}$$

$$\frac{1}{J^2}\frac{\partial J}{\partial h}=\sin\theta\frac{\partial^2 x}{\partial\psi\partial h}-\cos\theta\frac{\partial^2 y}{\partial\psi\partial h}.\tag{S.14}$$

The right-hand sides of eqs. (S.9) and (S.14) are the same; the pairs of eqs. (S.10) and (S.13) also has the same right-hand sides. Thus, we conclude that the functions $\theta(h,\psi)$ and $J(h,\psi)$ of h and ψ are related by

$$\frac{1}{\Phi(J)}\frac{\partial\theta}{\partial\psi}=\frac{1}{J^2}\frac{\partial J}{\partial h},\tag{S.15}$$

$$\frac{1}{J}\frac{\partial\theta}{\partial h}=-\frac{\Phi'(J)}{\Phi^2(J)}\frac{\partial J}{\partial\psi}.\tag{S.16}$$

3. The Cauchy-Riemann equations analogous to eqs. (S.15), (S.16)

To transform eqs. (S.15), (S.16) to the Cauchy-Riemann equations, we substitute the definition (3.2) of the function $\Phi(J)$:

$$\Phi(J)=\frac{J}{\left(1-J^2\right)^{1/2}},\quad \frac{d\Phi}{dJ}=\Phi'=\frac{1}{\left(1-J^2\right)^{3/2}},\tag{S.17}$$

in eqs. (S.15), (S.16):

$$\frac{\partial J}{\partial h}=\frac{J^2}{\Phi(J)}\frac{\partial \theta}{\partial \psi}=J\left(1-J^2\right)^{1/2}\frac{\partial \theta}{\partial \psi}, \tag{S.18}$$

$$\frac{\partial J}{\partial \psi}=-\frac{\Phi^2(J)}{J\Phi'(J)}\frac{\partial \theta}{\partial h}=-\frac{J^2\left(1-J^2\right)^{3/2}}{\left(1-J^2\right)J}\frac{\partial \theta}{\partial h}=-J\left(1-J^2\right)^{1/2}\frac{\partial \theta}{\partial h}. \tag{S.19}$$

To reduce eqs. (S.18), (S.19) to the Cauchy-Riemann equations, we need to eliminate the factors at the derivatives on the right hand sides of these equations. To do this, we introduce yet unknown function $t=t(J)$ and rewrite eqs. (S.18), (S.19) as

$$\frac{\partial t}{\partial h}=t'(J)\frac{\partial J}{\partial h}=\left[t'(J)J\left(1-J^2\right)^{1/2}\right]\frac{\partial \theta}{\partial \psi}, \tag{S.20}$$

$$\frac{\partial t}{\partial \psi}=t'(J)\frac{\partial J}{\partial \psi}=-\left[t'(J)J\left(1-J^2\right)^{1/2}\right]\frac{\partial \theta}{\partial h}. \tag{S.21}$$

This function $t=t(J)$ is chosen to turn the bracketed term into -1:

$$\left[t'(J)J\left(1-J^2\right)^{1/2}\right]=-1 \quad \Rightarrow \quad t'(J)=-\frac{1}{J\left(1-J^2\right)^{1/2}}. \tag{S.22}$$

Integrating this equation, we find

$$t=\operatorname{arccosh}\frac{1}{J}, \quad \Rightarrow J=\frac{1}{\cosh t}, \quad \Phi(J)=\frac{1}{\sinh t}. \tag{S.23}$$

Consequently, eqs. (S.20), (S.21) take on the Cauchy-Riemann form as

$$-\frac{\partial t}{\partial h}=\frac{\partial \theta}{\partial \psi}, \quad \frac{\partial t}{\partial \psi}=\frac{\partial \theta}{\partial h}. \tag{S.24}$$

Introducing the complex-valued functions $\chi=t+i\theta$ and $W=-h+i\psi$ the Cauchy-Riemann equations can be written in inverse form as

$$\frac{\partial h}{\partial t}=-\frac{\partial \psi}{\partial \theta}, \quad \frac{\partial \psi}{\partial t}=\frac{\partial h}{\partial \theta}. \tag{S.25}$$

We use this form in our analysis of minimal surfaces.

4. How to construct the minimal surface

Using (S.23) to replace J and $\Phi(J)$ in eqs. (S.4), we obtain

$$\frac{\partial x}{\partial h}=-\cos\theta\sinh t,\quad \frac{\partial x}{\partial \psi}=-\sin\theta\cosh t,$$
$$\frac{\partial y}{\partial h}=-\sin\theta\sinh t,\quad \frac{\partial y}{\partial \psi}=\cos\theta\cosh t. \tag{S.26}$$

We seek solutions $x(h,\psi)$, $y(h,\psi)$ as functions of the variables ξ,η. Using the chain rule, we have for the partial derivatives

$$\frac{\partial x}{\partial \xi}=\frac{\partial x}{\partial h}\frac{\partial h}{\partial \xi}+\frac{\partial x}{\partial \psi}\frac{\partial \psi}{\partial \xi},\quad \frac{\partial x}{\partial \eta}=\frac{\partial x}{\partial h}\frac{\partial h}{\partial \eta}+\frac{\partial x}{\partial \psi}\frac{\partial \psi}{\partial \eta},$$
$$\frac{\partial y}{\partial \xi}=\frac{\partial y}{\partial h}\frac{\partial h}{\partial \xi}+\frac{\partial y}{\partial \psi}\frac{\partial \psi}{\partial \xi},\quad \frac{\partial y}{\partial \eta}=\frac{\partial y}{\partial h}\frac{\partial h}{\partial \eta}+\frac{\partial y}{\partial \psi}\frac{\partial \psi}{\partial \eta}. \tag{S.27}$$

Substituting (S.26) and (5.2) for the partial derivatives on the right-hand sides of (S.27), we arrive at eqs. (6.3) – (6.4) in the main text:

$$\frac{\partial x}{\partial \xi}=\frac{H}{2K}\cos\theta\sinh t,\qquad \frac{\partial y}{\partial \xi}=\frac{H}{2K}\sin\theta\sinh t, \tag{S.28}$$

$$\frac{\partial x}{\partial \eta}=-\frac{H}{2K}\sin\theta\cosh t,\qquad \frac{\partial y}{\partial \eta}=\frac{H}{2K}\cos\theta\cosh t\ . \tag{S.29}$$

5. Non-uniqueness of surfaces Σ as shown by non-monotonicity of function $H(q)$.

The dependence $H(q)$ has been calculated by picking an auxiliary parameter q and substituting the calculated parameters m, K, K' defined by (5.7), (5.8) in (6.10) for H using the function χ from expression (5.5). The results are shown in Fig. S.1 by the solid curve for different n-sided polygonal frames: *a*) $n=3$, *b*) $n=4$, *c*) $n=5$. For each n-sided polygon, there is a maximum $H=H^*(n)$ at some critical value $q=q^*(n)$, labeled by the star in Figs. S.1*a*), *b*), *c*). Thus, no minimal surfaces exist for the separation distances greater than $H>H^*(n)$!

A non-monotonic behavior of the separation distance on the auxiliary parameter q suggests that for each separation distance $H\le H^*(n)$, we have two surfaces specified by two different q-values. Thus, the behavior of surfaces supported by polygonal frames is similar to that of the classical catenoid[3].

The difference between the classical catenoid and the studied surfaces is that the hole in the middle forming contour Γ is not circular for the polygonal frames. It is convenient to introduce a quantitative metric of roundness of this hole comparing the distances from points D

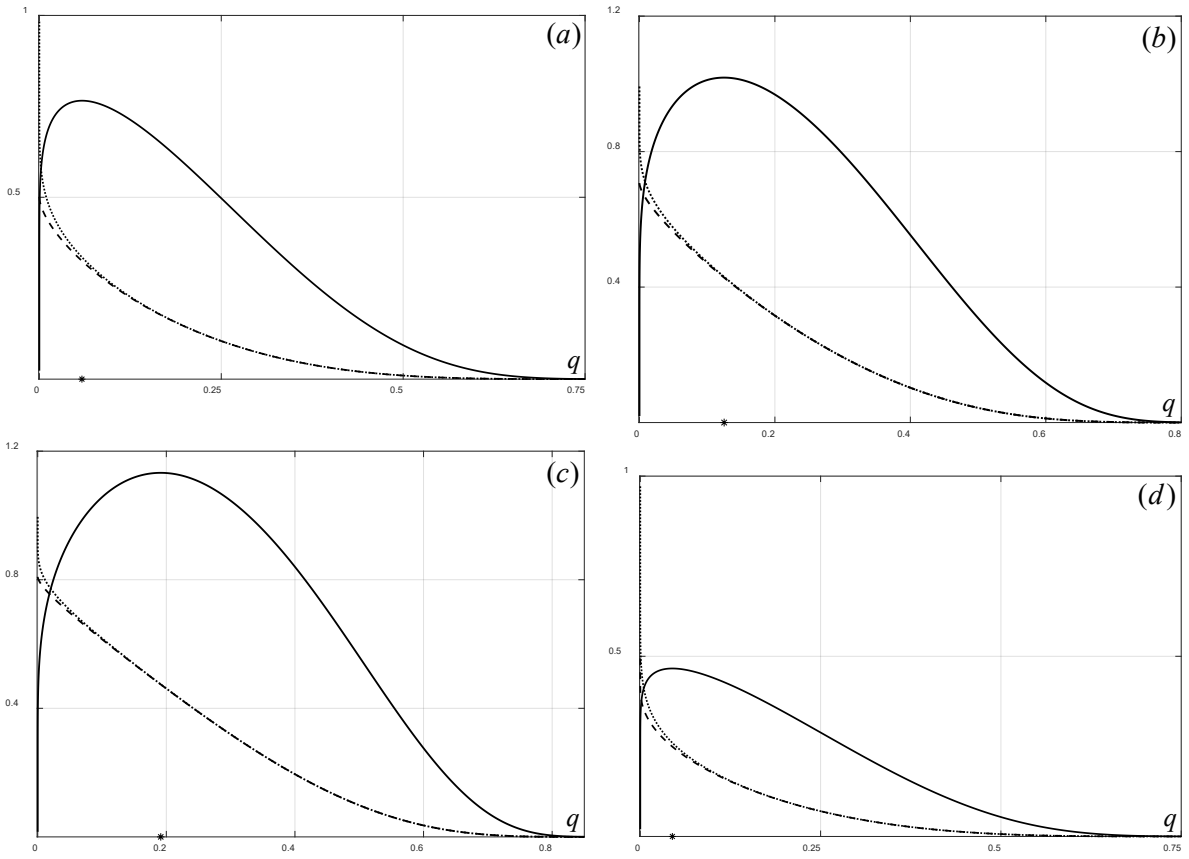

Fig. S.1. Dependence of parameters H (solid), R_D (dotted), and R_C (dashed) on auxiliary parameter q for surfaces without lamellae on n-sided frames: (*a*) $n=3$, (*b*) $n=4$, (*c*) $n=5$. (*d*) same dependence for surfaces with lamellae sitting on triangular equilateral frames $n=3$. The critical q corresponding to the maximal separation distance H are marked with stars.

and C to the central axis z: $R_D \equiv x_D$, $R_C \equiv y_C / \sin\beta_n$, Fig. 2(*a*). For the case of a surface without lamella, the dependences $R_D(q)$ and $R_C(q)$ on auxiliary parameter q follows from (6.8):

$$\begin{aligned} R_D &= \cos^2\beta_n - \frac{H}{2K}\left[\cos\beta_n \int_{-K}^{0} \sinh t\,\Big|_{\eta=K'} d\xi - \int_{0}^{K'} \sin\theta\,\Big|_{\xi=-K} d\eta\right], \\ R_C &= \frac{H}{2K\sin\beta_n} \int_{0}^{K'} \cos\theta\,\Big|_{\xi=-K} d\eta, \end{aligned} \tag{S.30}$$

where functions $t(\xi, K')$, $t(-K,\eta)$ and $\theta(-K,\eta)$ are defined by expression (5.5).

For the case of a surface with lamella, the dependences $R_D(q)$ and $R_C(q)$ on the auxiliary parameter q follows from (6.15):

$$R_D = \cos^2\beta_n - \frac{H}{2K}\left[\cos\beta_n \int_{-K}^{0} \sinh t\,\Big|_{\eta=K'} d\xi - \cosh t_\Gamma \int_{0}^{K'} \sin\theta\,\Big|_{\xi=-K} d\eta\right],$$
$$R_C = \frac{H\cosh t_\Gamma}{2K\sin\beta_n}\int_{0}^{K'} \cos\theta\,\Big|_{\xi=-K} d\eta, \tag{S.31}$$

where functions $t(\xi,K')$, $t(-K,\eta)$ and $\theta(-K,\eta)$ are defined by expression (5.6).

In Fig. S.1, we plot $R_D(q)$ and $R_C(q)$ by the dotted and dashed lines for *a*) $n=3$, *b*) $n=4$, *c*) $n=5$. These dependencies are monotonic, so hence each surface specified by the given q-parameter has only one specific $R_D(q)$ or $R_C(q)$ value. We can also specify the critical $R_D^*(n)$ corresponding to the critical $q=q^*(n)$ where the separation distance reaches its maximum $H^*(n)$.

6. Derivation of expression (5.5).

Using (5.3), (5.4), we write for $\chi(\zeta)$:

$$\chi(\zeta) = -i\frac{2\beta_n}{\pi}\arcsin\left\{\omega_B\left[1-\mathrm{sn}^{-2}(\zeta\,|\,m)\right]^{1/2}\right\} \tag{S.32}$$

where $\omega_B = -1/\sqrt{1-m}$.

The complex valued arcsine function is multivalued therefore, to select a single valued branch of this function, we rewrite the arcsine function using its logarithmic representation as[4]

$$\begin{aligned}
\chi(\zeta) &= -\frac{2\beta_n}{\pi}\ln\left\{\left[1-\omega_B^2+\omega_B^2\,\mathrm{sn}^{-2}(\zeta\,|\,m)\right]^{1/2} - \omega_B\left[\mathrm{sn}^{-2}(\zeta\,|\,m)-1\right]^{1/2}\right\} = \\
&= -\frac{2\beta_n}{\pi}\ln\left\{\left[1-m_1^{-1}+m_1^{-1}\,\mathrm{sn}^{-2}(\zeta\,|\,m)\right]^{1/2} + m_1^{-1/2}\left[\mathrm{sn}^{-2}(\zeta\,|\,m)-1\right]^{1/2}\right\} = \\
&= -\frac{2\beta_n}{\pi}\ln\left\{\left[m_1-1+\mathrm{sn}^{-2}(\zeta\,|\,m)\right]^{1/2} + \left[\mathrm{sn}^{-2}(\zeta\,|\,m)-1\right]^{1/2}\right\} + \frac{\beta_n}{\pi}\ln m_1 = \\
&= -\frac{2\beta_n}{\pi}\ln\left\{\left[\mathrm{sn}^{-2}(\zeta\,|\,m)-m\right]^{1/2} + \left[\mathrm{sn}^{-2}(\zeta\,|\,m)-1\right]^{1/2}\right\} + \frac{\beta_n}{\pi}\ln(1-m),
\end{aligned} \tag{S.33}$$

where we used $m_1 = 1-m$. Pulling out the factor, $2\beta_n/\pi$, the last line of expression (S.33) can be rewritten as

$$\chi(\zeta) = \frac{2\beta_n}{\pi}\left\{\ln\sqrt{1-m} - \ln\left(\left[\mathrm{sn}^{-2}(\zeta\,|\,m)-m\right]^{1/2} - \left[\mathrm{sn}^{-2}(\zeta\,|\,m)-1\right]^{1/2}\right)\right\}. \tag{S.34}$$

where the branches of logarithm and square root are fixed by choosing the correspondence of points A_1 in the ζ- and χ-planes and have zero argument at the A_1D boundary where the Jacobi elliptic function $\mathrm{sn}(\zeta\,|\,m)$ is real valued (see Fig. 4*c*). The selection of the "$\pm$" signs for

the second logarithm in (S.34) is decided in favor of the negative sign to ensure the correspondence of points A_1 in planes ζ and χ.

The function $\mathrm{sn}(\zeta\,|\,m)$ goes to zero at the point A_1. Therefore, in the vicinity of this point A_1, the right-hand side of (S.34) has to be calculated with a special care. The following asymptotic approximation is used there:

$$
\begin{aligned}
&|\,\mathrm{sn}(\zeta\,|\,m)\,| \ll 1: \quad \chi(\zeta) = -\frac{2\beta_n}{\pi}\ln\left\{\left[1-\omega_B^2+\omega_B^2\,\mathrm{sn}^{-2}(\zeta\,|\,m)\right]^{1/2}-\omega_B\left[\mathrm{sn}^{-2}(\zeta\,|\,m)-1\right]^{1/2}\right\} = \\
&= -\frac{2\beta_n}{\pi}\ln\left\{\omega_B\mathrm{sn}^{-1}(\zeta\,|\,m)\left[1-\left(1-\omega_B^{-2}\right)\mathrm{sn}^2(\zeta\,|\,m)\right]^{1/2}-\omega_B\mathrm{sn}^{-1}(\zeta\,|\,m)\left[1-\mathrm{sn}^2(\zeta\,|\,m)\right]^{1/2}\right\} \approx \\
&\approx -\frac{2\beta_n}{\pi}\ln\left\{\omega_B\mathrm{sn}^{-1}(\zeta\,|\,m)\left[1-\left(1-\omega_B^{-2}\right)\frac{\mathrm{sn}^2(\zeta\,|\,m)}{2}\right]-\omega_B\mathrm{sn}^{-1}(\zeta\,|\,m)\left[1-\frac{\mathrm{sn}^2(\zeta\,|\,m)}{2}\right]\right\} = \\
&= -\frac{2\beta_n}{\pi}\ln\left[\frac{\mathrm{sn}(\zeta\,|\,m)}{2\omega_B}\right]
\end{aligned}
\tag{S.35}
$$

Thus, we obtain

$$
|\,\mathrm{sn}(\zeta\,|\,m)\,| \ll 1: \quad \chi(\zeta) \approx -\frac{2\beta_n}{\pi}\ln\left[\frac{\mathrm{sn}(\zeta\,|\,m)}{2\omega_B}\right]. \tag{S.36}
$$

7. Calculation of the surface area defined by expression (7.5).

The surface area depends on the integral taken over the domain Ω_ζ:

$$
J = \iint\limits_{\Omega_\zeta} \cosh^2 t(\xi,\eta)\,d\xi d\eta, \tag{S.37}
$$

where $t(\xi,\eta) = \mathrm{Re}\,\chi(\zeta)$, and the function $\chi(\zeta)$ is specified by expression (5.5).

At the point A_1 (see Fig. S.2), the integral (S.37) has an integrable singularity which, however, MATLAB toolboxes cannot adequately handle leading to unacceptable accuracy of numeric integration. After discovering this inaccuracy, we conducted the following asymptotic analysis to achieve acceptable numerical results.

Consider a small ε-vicinity of point A_1, corresponding to a circular quadrant Ω_I of radius $\varepsilon \ll 1$ (Fig. S.2). The rest of domain Ω_ζ will be denoted by Ω_{II}; therefore, the domain of integration in (S.37) is $\Omega_\zeta = \Omega_I \cup \Omega_{II}$.

The integral J is represented as

$$
J = J_I + J_{II}, \quad J_{I,II} = \iint\limits_{\Omega_{I,II}} \cosh^2 t(\xi,\eta)\,d\xi d\eta\,. \tag{S.38}
$$

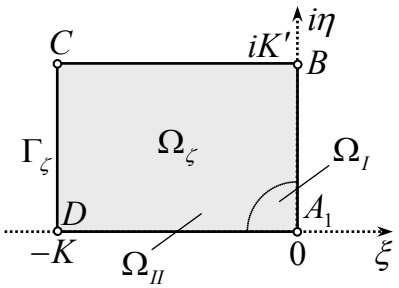

Fig. S.2. The domain Ω_ζ of integration in eq. (S.32); it is constituted of an infinitesimally small circular quadrant Ω_I of radius $\varepsilon \ll 1$ and domain Ω_{II}.

We are going to show that the first integral J_I can be asymptotically estimated as

$$J_I = \iint_{\Omega_I} \cosh^2 t(\xi,\eta)\, d\xi d\eta \; = 3\pi \left[\frac{\varepsilon}{16(1-m)}\right]^{2/3} + O\left(\varepsilon^2\right), \tag{S.39}$$

while the second integral J_{II} does not have any singularities and can be safely evaluated by the MATLAB subroutines.

Asymptotic analysis of integral J_I. First, we have to evaluate t using its definition as the real part of the function χ from (5.5):

$$\chi(\zeta) = t + i\theta = \frac{2\beta_n}{\pi}\left\{\ln\sqrt{1-m} - \ln\left(\left[\mathrm{sn}^{-2}\left(\zeta \mid m\right) - m\right]^{1/2} - \left[\mathrm{sn}^{-2}\left(\zeta \mid m\right) - 1\right]^{1/2}\right)\right\}. \tag{S.40}$$

In the quadrant Ω_I of radius $\varepsilon \ll 1$, the modulus of ζ is less than ε:

$$\Omega_I: \quad |\zeta| < \varepsilon \ll 1. \tag{S.41}$$

Therefore, for the Jacobi function sn, we use the asymptotic representation[5]

$$\Omega_I: \quad \mathrm{sn}\,\zeta = \zeta - \frac{1+m}{6}\zeta^3 + O\left(|\zeta|^5\right). \tag{S.42}$$

Thus, the function $\mathrm{sn}^{-2}\zeta$ needed to calculate the bracketed terms in the logarithm in (S.40) is estimated as

$$\Omega_I: \quad \mathrm{sn}^{-2}\zeta = \left[\zeta - \frac{1+m}{6}\zeta^3 + O\left(|\zeta|^5\right)\right]^{-2} = \zeta^{-2}\left[1 + \frac{1+m}{3}\zeta^2 + O\left(|\zeta|^4\right)\right]. \tag{S.43}$$

In the multivalued function $\left(\zeta^{-2}\right)^{1/2} = \pm\zeta^{-1}$ we select the branch specified in eq. (5.5): $\left(\zeta^{-2}\right)^{1/2} = \{-\zeta^{-1}\}$. Therefore, the difference of the bracketed terms in the second logarithm in (S.40) can be asymptotically estimated as

$$\Omega_I:\ \left[\mathrm{sn}^{-2}\zeta-m\right]^{1/2}-\left[\mathrm{sn}^{-2}\zeta-1\right]^{1/2}=\left\{-\zeta^{-1}\right\}\left[1+\frac{1+m}{3}\zeta^2+O\left(|\zeta|^4\right)-m\zeta^2\right]^{1/2}-$$
$$-\left\{-\zeta^{-1}\right\}\left[1+\frac{1+m}{3}\zeta^2+O\left(|\zeta|^4\right)-\zeta^2\right]^{1/2}=-\zeta^{-1}\left[1+\frac{1+m}{6}\zeta^2-\frac{m}{2}\zeta^2+O\left(|\zeta|^4\right)\right]+ \quad \text{(S.44)}$$
$$+\zeta^{-1}\left[1+\frac{1+m}{6}\zeta^2-\frac{1}{2}\zeta^2+O\left(|\zeta|^4\right)\right]=-\frac{1-m}{2}\zeta+O\left(|\zeta|^3\right).$$

Substituting the estimate (S.44) in (S.40), and remembering that $\beta_n=\pi/n$, we obtain

$$\Omega_I:\quad \chi(\zeta)=\frac{2\beta_n}{\pi}\ln(1-m)^{1/2}-\frac{2\beta_n}{\pi}\ln\left\{-\frac{1-m}{2}\zeta\left[1+O\left(|\zeta|^2\right)\right]\right\}= \quad \text{(S.45)}$$
$$=\ln\left(-\zeta\right)^{-2/n}+\ln\left(\frac{4}{1-m}\right)^{1/n}+\ln\left[1+O\left(|\zeta|^2\right)\right].$$

Therefore, extracting the real part $t\left(\xi,\eta\right)=\mathrm{Re}\,\chi(\zeta)$, we have

$$\Omega_I:\quad t(\xi,\eta)=\ln\left(\xi^2+\eta^2\right)^{-1/n}+\ln\left(\frac{4}{1-m}\right)^{1/n}+\ln\left[1+O\left(|\zeta|^2\right)\right]. \quad \text{(S.46)}$$

Thus, the integrand in (S.39) is evaluated as

$$\Omega_I:\quad \cosh^2 t(\xi,\eta)=\frac{1}{4}\left\{e^{2t}+e^{-2t}+2\right\}=\frac{1}{4}\left\{\left(\xi^2+\eta^2\right)^{-2/n}\left(\frac{4}{1-m}\right)^{2/n}\left[1+O\left(|\zeta|^2\right)\right]+\right. \quad \text{(S.47)}$$
$$\left.+\left(\xi^2+\eta^2\right)^{2/n}\left(\frac{1-m}{4}\right)^{2/n}\left[1+O\left(|\zeta|^2\right)\right]+2\right\}=\frac{\left(\xi^2+\eta^2\right)^{-2/n}}{4^{(1-2/n)}(1-m)^{2/n}}+2+O\left(|\zeta|^{2/n}\right).$$

Expression (S.47) allows us to estimate the integral (S.39) as

$$J_I=\frac{1}{4^{(1-2/n)}(1-m)^{2/n}}\iint\limits_{\Omega_I}\left(\xi^2+\eta^2\right)^{-2/n}d\xi d\eta+\iint\limits_{\Omega_I}\left[2+O\left(\varepsilon^2\right)\right]d\xi d\eta\,. \quad \text{(S.48)}$$

On the right-hand side of (S.48), the second integral over the quadrant Ω_I is calculated straightforwardly as $\pi\varepsilon^2/2+O(\varepsilon^4)$. The first integral is evaluated by introducing a polar system of coordinates $\rho=|\zeta|$ and $\sigma=\arg\zeta$, and we finally obtain:

$$J_I=\frac{1}{4^{(1-2/n)}(1-m)^{2/n}}\int\limits_{\pi/2}^{\pi}\int\limits_{0}^{\varepsilon}\rho^{-4/n}\rho\,d\rho\,d\sigma+\frac{\pi\varepsilon^2}{2}+O\left(\varepsilon^4\right)=\frac{\pi n\varepsilon^{2-4/n}}{4^{(2-2/n)}(n-2)(1-m)^{2/n}}+O\left(\varepsilon^2\right). \quad \text{(S.49)}$$

In the lamella case, one needs to add a real constant t_Γ in the right hand side of (S.46); consequently, the right hand side of (S.49) needs to be multiplied by the real valued factor e^{2t_Γ}.

This formula leads us to the estimate (S.39). In the MATLAB calculations, we used $\varepsilon=10^{-4}$, therefore the accuracy of these calculations is $O(\varepsilon^2)=10^{-8}$.

8. Numeric calculations.

MATLAB R2017 has been used for numeric calculations of the analytic results. To calculate the Jacobi function $\mathrm{sn}(\zeta \,|\, m)$ of the complex valued variable $\zeta = \xi + i\eta$, we used the following representation 16.21.2 from Ref.[4]

$$\mathrm{sn}(\zeta \,|\, m) = \frac{\mathrm{sn}(\xi \,|\, m)\,\mathrm{dn}(\eta \,|\, m_1) + i\,\mathrm{cn}(\xi \,|\, m)\,\mathrm{dn}(\xi \,|\, m)\,\mathrm{sn}(\eta \,|\, m_1)\,\mathrm{cn}(\eta \,|\, m_1)}{\mathrm{cn}^2(\eta \,|\, m_1) + m\,\mathrm{sn}^2(\xi \,|\, m)\,\mathrm{sn}^2(\eta \,|\, m_1)}, \qquad \text{(S.50)}$$

where

$$m_1 = 1 - m \qquad \text{(S.51)}$$

and the Jacobi functions sn, cn, dn of the real valued arguments ξ and η were calculated using the MATLAB functions "ellipj".

When the auxiliary parameter q changes from 0 to 1, the parameter m defined by (5.7), also changes from 0 to 1. When q is small, $q \le e^{-\pi}$, we never experienced any problem in calculating these integrals. The minimal value that has been used in our calculations was $q = 10^{-100}$.

When the parameter $m(q)$ approaches 1, it does so much steeper than a linear function $m \propto q$. For example, at $q = 0.7$, we have $m \approx 1 - 10^{-11}$, and, accordingly, $m_1 \sim 10^{-11}$. Thus, the accuracy of calculations of the Jacobi functions and their integrals with $m_1 = 1 - m$ may be lost. For example, to calculate integrals from Sect. 5 involving function $\chi(\zeta) = t + i\theta$, one can use (5.5) or (5.6). Since m goes to 1 as q goes to 1, the right hand sides of these equations behave as $\ln(0) - \ln(0)$.

To resolve this uncertainty, one can limit the range of change of the auxiliary parameter q to that where the formulas (5.5), (5.6) remain non-singular. We used $q \le 0.7$. This strategy has been applied to calculate the area S when we changed q from 0 to $q = 0.55$. When $q > 0.55$, the curves *2* and *2′* in Fig. 7 practically coincide with the dashed curve corresponding to the two flat separated lamellae.

This strategy has to be adjusted when one needs to determine the dependencies $R_C(H)$, $R_D(H)$ for $n \ge 4$. Thus, to reach the region where the solid curves closely approach the dashed ones in Fig. S1(*b*), (*c*), we increased the range of change of the auxiliary parameter to $q \le 0.85$. The following steps have been applied to increase the upper limit of q:

1) Calculating m_1 when $q > e^{-\pi}$. We introduce the complementary Jacobi nome q_1, see 17.3.19 from Ref.[4]

$$q_1 = \exp\left(\frac{\pi^2}{\ln q}\right). \tag{S.52}$$

Then m_1 is calculated using 16.38.5, 16.38.7 and 17.3.17, 17.3.18 from Ref. [4]

$$m_1 = 16q_1\left[1+\sum_{n=1}^{\infty} q_1^{n^2+n}\right]^4\left[1+2\sum_{n=1}^{\infty} q_1^{n^2}\right]^{-4}. \tag{S.53}$$

The parameter m is obtained from (S.51).

2) Calculating $t(\xi,\eta)$ at the boundary BC. To calculate the first integral defining R_D in (6.14), we derive a new formula for $t(\xi,\eta) = \mathrm{Re}\,\chi(\zeta)$ at BC. Using the boundary condition (4.3) at BC and the first expression (5.4), we have

$$BC: \quad \omega = \sin\left[\frac{\pi}{2\beta_n}\left(-\beta_n + it\right)\right] = -\cos\left(i\frac{\pi t}{2\beta_n}\right) = -\cosh\left(\frac{\pi t}{2\beta_n}\right). \tag{S.54}$$

On the other hand, the following expression $\omega = m_1^{-1/2}\left[1-\mathrm{sn}^{-2}(\zeta\,|\,m)\right]^{1/2}$ is derived from (5.3). At BC, the single valued branch of the square root is chosen as

$$BC: \quad \omega = -\sqrt{\frac{1-\mathrm{sn}^{-2}\left(\zeta\,|\,m\right)}{m_1}}, \tag{S.55}$$

where the function $\mathrm{sn}\left(\zeta\,|\,m\right)$ at BC is written using 16.8.1 from Ref.[4] as

$$BC: \quad \mathrm{sn}\left(\zeta\,|\,m\right) = \mathrm{sn}\left(\xi + iK'\,|\,m\right) = \frac{1}{\sqrt{m}}\mathrm{ns}\left(\xi\,|\,m\right),$$

and using 16.3.1 and 16.9.1 from Ref.[4], we obtain

$$BC: \quad 1-\mathrm{sn}^{-2}\left(\zeta\,|\,m\right) = 1-\frac{m}{\mathrm{ns}^2\left(\xi\,|\,m\right)} = 1-m\,\mathrm{sn}^2\left(\xi\,|\,m\right) = \mathrm{dn}^2\left(\xi\,|\,m\right), \tag{S.56}$$

where $\mathrm{ns}\left(\xi\,|\,m\right)$ and $\mathrm{dn}\left(\xi\,|\,m\right)$ – is another pair of the Jacobi functions.

Substituting (S.56) in (S.55), we obtain

$$BC: \quad \omega = -\frac{\mathrm{dn}\left(\xi\,|\,m\right)}{\sqrt{m_1}}, \tag{S.57}$$

Comparing (S.54) and (S.57), we have

$$BC: \quad \cosh\left(\frac{\pi t}{2\beta_n}\right) = \frac{\mathrm{dn}\left(\xi\,|\,m\right)}{\sqrt{m_1}}. \tag{S.58}$$

Solving (S.58) for t, we have

$$BC: \quad t(\xi, K') = \frac{2\beta_n}{\pi} \operatorname{arccosh}\left[\frac{\operatorname{dn}(\xi \mid m)}{\sqrt{m_1}}\right]. \tag{S.59}$$

This is a new representation of $t(\xi,\eta) = \operatorname{Re}\chi(\zeta)$ at BC. For the lamella case, the constant t_Γ has to be added to the right hand side of (S.59):

$$BC: \quad t(\xi, K') = \frac{2\beta_n}{\pi} \operatorname{arccosh}\left[\frac{\operatorname{dn}(\xi \mid m)}{\sqrt{m_1}}\right] + t_\Gamma. \tag{S.60}$$

The formulas (S.59), (S.60) are convenient to calculate for any $m_1 > 0$.

3) Calculating $\theta(\xi,\eta)$ at CD. To calculate the integrals in expressions for R_D and R_C, (6.14), we introduce a representation alternative to (5.5), (5.6) at CD for function $\theta(\xi,\eta) = \operatorname{Im}\chi(\zeta)$. Using the boundary condition (4.2) at CD and the first expression (5.4), we have

$$CD: \quad \omega = -\sin\left(\frac{\pi\theta}{2\beta_n}\right). \tag{S.61}$$

On the other hand, from (5.3) similarly to the derivation of (S.55), we have on CD:

$$CD: \quad \omega = -\sqrt{\frac{1-\operatorname{sn}^{-2}(\zeta \mid m)}{m_1}}. \tag{S.62}$$

For the Jacobi functions $\operatorname{sn}(\zeta \mid m)$ and $\operatorname{cd}(i\eta \mid m)$, the following representation holds true (we used 16.8.1, 16.3.1, 16.20.2, 16.20.3, 16.3.4 from Ref.[4])

$$\begin{aligned} CD: \quad & \operatorname{sn}(\zeta \mid m) = \operatorname{sn}(-K + i\eta \mid m) = -\operatorname{cd}(i\eta \mid m) = \\ & = -\frac{\operatorname{cn}(i\eta \mid m)}{\operatorname{dn}(i\eta \mid m)} = -\frac{\operatorname{nc}(\eta \mid m_1)}{\operatorname{dc}(\eta \mid m_1)} = -\operatorname{nd}(\eta \mid m_1), \end{aligned} \tag{S.63}$$

Applying the known relations between these Jacobi functions[4], the function $1-\operatorname{sn}^{-2}(\zeta \mid m)$ is represented at CD as 16.3.3, 16.9.1

$$CD: \quad 1-\operatorname{sn}^{-2}(\zeta \mid m) = 1 - \frac{1}{\operatorname{nd}^2(\eta \mid m_1)} = 1 - \operatorname{dn}^2(\eta \mid m_1) = m_1 \operatorname{sn}^2(\eta \mid m_1), \tag{S.64}$$

Substituting (S.64) in (S.62), we obtain the boundary condition in the form

$$CD: \quad \omega = -\operatorname{sn}(\eta \mid m_1), \tag{S.65}$$

Comparing the right hand sides of (S.61) and (S.65), we write

$$CD: \quad \sin\left(\frac{\pi\theta}{2\beta_n}\right)=\mathrm{sn}\left(\eta\,|\,m_1\right). \tag{S.66}$$

Solving (S.66) for θ, we obtain a representation of $\theta(\xi,\eta)$ at CD as

$$CD: \quad \theta(-K,\eta)=\frac{2\beta_n}{\pi}\arcsin\left[\,\mathrm{sn}\left(\eta\,|\,m_1\right)\right]. \tag{S.67}$$

This expression is applicable for the lamella case as well. For calculating θ at any small, the formula (S.67) is very convenient to use.

4) Calculating the minimal surfaces. Calculating the shape $h(x,y)$, one needs to evaluate the integrals (6.11) where the multivalued functions of logarithm and square root are involved, see (5.5), (5.6). To evaluate the formulas (5.5), (5.6), the MATLAB logarithm and square roots were used. To confirm that MATLAB uses the correct single valued branches, we have checked the value of $\chi(\zeta)$ at A_1D. After checking the validity of t and $\theta=0$, at the boundary A_1D, see Fig. 3(*b*), the same formulas were used for calculating these function in the domain Ω_ζ. Calculating the integrals (6.11) in the entire domain Ω_ζ, we never observed any jumps between the single valued branches of these multivalued functions which could result in some defects on the obtained surface. Otherwise, we would change the single valued branches by adding either $\pm 2\pi i$ to the logarithm function or changing the sign to "–" of square root function. Thus, the integrals (6.11) were calculated without any difficulties. The point A_1 has to be excluded from the integration nodes because t goes to infinity at A_1, $t\to\infty$. There is no need to evaluate these integrals at A_1 because all the functions are known there: $x=1$, $y=0$, $h=0$.

9. The process of fitting experimental data to the theoretical predictions.

In the theory, the triangle $A_1A_2A_3$ is equilateral. The frames $A_1^{\square}A_2^{\square}A_3^{\square}$ made of wires cannot be made equilateral. Therefore we face two challenges: *a*) how to find an apparently equilateral frame which provides the best fit with the theory and place the center of theoretical triangle with respect to experimental; and *b*) how should we define the scaling factor $|OA_1|$ to get the best fit with the theory?

The theoretical critical contour Γ^* corresponding to the critical separation distance H^* is a planar curve characterized by 3-fold rotational symmetry: it is mirror-symmetric with respect to the x-axis and preserves the shape after rotation of the x-axis by the $2\pi/3$ and $4\pi/3$ angles around the z-axis. The point of intersection of the axes of symmetry, point O, is the geometrical center of this contour Γ^* as well as the center of equilateral triangle $A_1A_2A_3$. Considering the

theoretical contour Γ^* as a heavy thread, the point O, the geometrical center of this thread, can be calculated as the center of mass of this thread. Following this idea, the coordinates of point O are calculated by the formula

$$\mathbf{r}_O = \frac{\sum_{k=1}^{N-1}\left(\mathbf{r}_{k+1}+\mathbf{r}_k\right)\left|\mathbf{r}_{k+1}-\mathbf{r}_k\right| + \left(\mathbf{r}_1+\mathbf{r}_N\right)\left|\mathbf{r}_1-\mathbf{r}_N\right|}{2\left(\sum_{k=1}^{N-1}\left|\mathbf{r}_{k+1}-\mathbf{r}_k\right| + \left|\mathbf{r}_1-\mathbf{r}_N\right|\right)}, \tag{S.68}$$

where a set of data points N with coordinates $\mathbf{r}_n = (x_n, y_n)$, $n = 1,...,N$, taken using ImageJ from the photograph of the innermost experimental contour closest to the critical experimental Γ^*. This critical experimental contour is very difficult to identify, so the closest possible contour has been used for the fitting with the theory.

As soon as the position of center O is found, we can measure the distances $|OA_1^{\square}|$, $|OA_2^{\square}|$, $|OA_3^{\square}|$.

As the scaling factor $|OA_1|$ we have tried to use *a*) the mean value $|OA_1| = (1/3)\{|OA_1^{\square}| + |OA_2^{\square}| + |OA_3^{\square}|\}$, *b*) the maximum, $|OA_1| = \max\{|OA_1^{\square}|, |OA_2^{\square}|, |OA_3^{\square}|\}$ and *c*) the minimum $|OA_1| = \min\{|OA_1^{\square}|, |OA_2^{\square}|, |OA_3^{\square}|\}$.

Checking all these methods, we found that the best fit of the experimental profiles is provided by the scaling factor

$$|OA_1| = \min\left\{|OA_1^{\square}|, |OA_2^{\square}|, |OA_3^{\square}|\right\} \tag{S.69}$$

Bibliography

1. Chaplygin, S. A., Gas jets. *Uchenie Zapiski Imperatorskogo Moskovskogo Universiteta* **1904,** *21*, 1-121.
2. Chaplygin, S. A., Gas Jets. Translated by Reiss, S. ed.; NASA, Ed. National Advisory Commitee for Aeronautics: 2009; pp 1-115.
3. Arfken, G. B.; Weber, H. J.; Harris, F. E., *Mathematical Methods for Physicists*. 7th Edition ed.; Elsevier Academic Press: New York, 2012; p 1220.
4. Abramowitz, M.; Stegun, I. A., *Handbook of Mathematical Functions: with Formulas, Graphs, and Mathematical Tables*. 9th ed.; Dover Publications: New York, 1965; p 1046.
5. Whittaker, E. T.; Watson, G. N., *A course of modern analysis.* 4th ed.; Cambridge University Press: New York, 1996; p 620.